

Induction Machines limits Identification During Abnormal Conditions Using an Optimization Algorithm

Mohammed Alqahtani

Electrical Engineering Department
University of South Florida
Tampa, FL 33620, USA

Email: mohammed23@mail.usf.edu

Zhixin Miao

Electrical Engineering Department
University of South Florida
Tampa, FL 33620, USA

Email: zmiao@usf.edu

Lingling Fan

Electrical Engineering Department
University of South Florida
Tampa, FL 33620, USA

Email: linglingfan@usf.edu

Abstract—Steady-state calculation for a system with induction motor loads is challenging due to motor loads' characteristics. The objective of this paper is to find steady-state variables and operation limits of a system with induction motors using advanced computing tools, e.g., YALMIP. This is achieved through optimization problem formulating and solving. The proposed formulations can accurately identify the maximum load torque limit for induction motor during the occurrence of balanced and unbalanced voltage dip, the minimal voltage level a motor can handle for a given load torque, and state variables of a system under certain operating conditions. Solutions from the optimization problems are validated using electromagnetic transient (EMT) simulation results.

Index Terms—Three-Phase Induction Motors, voltage unbalance, power quality.

NOMENCLATURE

$\omega_e, \omega_r, \omega_m$ Stator, rotor, and rotating angular frequency.
 $P_{ag}, P_{ag}^p, P_{ag}^n$ Net, positive, negative air gap power.
 $T_{em}, T_{em}^p, T_{em}^n$ Net, positive, negative electromagnetic torque.
 I_s^n, I_r^n Stator and rotor negative sequence current.
 I_s^p, I_r^p Stator and rotor positive sequence current.
 R_g, X_g line resistance and reactance.
 R_r, X_r Rotor resistance and reactance.
 R_s, X_s Stator resistance and reactance.
 s , poles Slip, Poles.
 V_g^p, V_g^n Positive and negative sequence voltage of the grid.
 V_t^p, V_t^n Positive and negative sequence voltage of the motor.
 X_m Magnetizing reactance.

I. INTRODUCTION

Induction motors are widely used in the industry for their versatility and economic advantages [1], [2]. Three-phase induction motors are 80% of the industrial load [3]. Therefore, the performance of this type of machine under non-ideal conditions has been investigated and address in previous literature [3]–[11]. The harmonic impact on the induction machine is investigated in [7]. The presence of the harmonics increases

the temperature of the machine. In [6], the motor performance during short interruptions of the supply is studied. Short interruptions could cause mechanical shock to the induction motor. While overvoltage shortens the life of the motor, undervoltage cases the motor to heat and reduces its speed.

Another type of the power quality problems that cause several issues to the performance of the three-phase induction motor is the unbalance voltage supply. Several studies have been conducted to examine the different impacts of the unbalanced voltage supply since the 1950s [8]. In addition to the efficiency reduction of the motor, protection difficulties can be introduced by small unbalances in line voltages [5].

Temperature rise, which minimizes the life of the motor, is another issue caused by the unbalance voltage condition. In [10], the heat impact of the negative-sequence current is examined. A small negative-sequence stator voltage will cause a large negative-sequence current, which leads to more heating. In addition, the presence of the negative sequence causes vibration which may lead to sever mechanical issues.

Unbalanced motor voltages will induce unbalanced currents which contain positive and negative sequence components. The positive current component will produce a torque that is in the direction of field of the positive-sequence current. Meanwhile, the negative current component will induces a reversing torque that is in the opposite direction of the positive-sequence magnetic field. Hence, the maximum average torque can be achieve by the machine is reduced due to unbalance. Further, the interactions between the two fields of different sequences and produced by stator currents and rotor currents introduces pulsating torque and motor noise [12].

With more smart building integrated into power grids and given that induction motor loads are major components of smart building [13], interest on steady-state analysis of a system with induction motor loads rekindled. Compared to a half century ago, we now possess more advanced computing tools to conduct analysis. Thus, the objective of this paper is to conduct steady-state analysis of induction motor operation using advanced computing tools, e.g., YALMIP [14], a MATLAB toolbox for optimization. In this paper, the steady-

state variables of the motor under certain conditions are found by means of solving nonlinear equations. An optimization problem is formulated to find the maximum load torque a motor can handle during balanced and unbalanced voltage dip. Moreover, the minimal grid voltage that a motor can handle to serve a given torque is found using the optimization approach. The results show that the proposed algorithm can accurately identify the motor variables and limits.

The rest of the paper is organized as follows. Section II and Section III present the steady-state equivalent circuit of an induction motor and the steady-state variables calculation. Three case studies, namely, (i) finding the motor state variables during unbalanced voltage condition, (ii) maximum torque that a motor can handle during unbalanced voltage dip, and (iii) minimal grid voltage a motor can handle for a given torque, are given in Section IV. The analysis results are confirmed by simulation results from MATLAB/SimPowerSystems. The conclusion is presented in section V.

II. EQUIVALENT CIRCUITS OF AN INDUCTION MOTOR

During unbalanced voltage condition, a three-phase induction motor can be represented by two equivalent steady-state circuits: positive- and negative-sequence circuits. The zero-sequence is neglected as the zero-sequence stator current does not setup a magnetic field. Hence there is no induction on the rotor side, nor there will be torque generated. If the circuit connecting the motor to the grid is taken into account (as in Fig. 1), the positive- and negative-sequence equivalent circuits will be given in Fig. 2. The core loss is neglected since it is very low compared to the rotor and the stator copper losses.

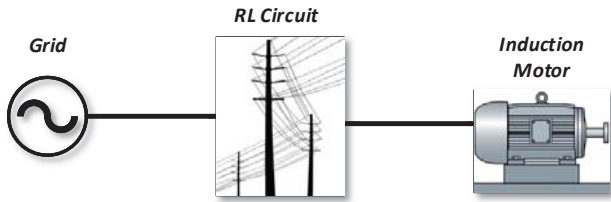


Fig. 1: System Configuration.

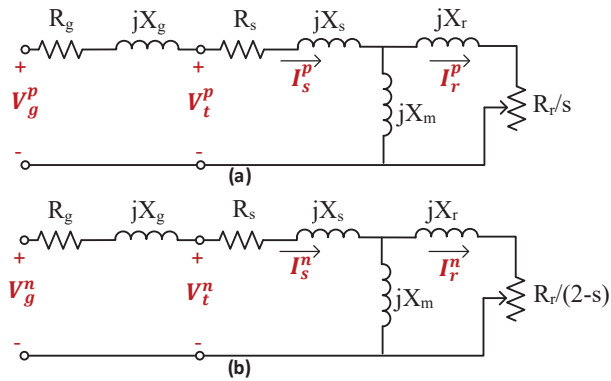


Fig. 2: Equivalent circuit. (a) positive-sequence circuit (b) negative-sequence circuit.

In order to find the nine steady-state variables including stator positive- and negative-sequence currents (notated as $I_s^p \angle \phi_s^p$,

$I_s^n \angle \phi_s^n$), rotor positive- and negative-sequence currents, (notated as $I_r^p \angle \phi_r^p$, $I_r^n \angle \phi_r^n$) and machine slip (notated as s) for the system in Fig. 1 for a given grid voltage and motor torque, nine equations should be considered. Difficulties are introduced due to the non-linearity of these equations. In section III, detailed formulation is provided to solve the problem through an advanced computing tool (YALMIP [14]).

The two equivalent circuits can be expressed by four equations, shown in (1).

$$-V_g^p \angle \theta_g^p + (R_s + R_g + j(X_s + X_m + X_g))I_s^p \angle \phi_s^p - jX_m I_r^p \angle \phi_r^p = 0 \quad (1a)$$

$$-V_g^n \angle \theta_g^n + (R_s + R_g + j(X_s + X_m + X_g))I_s^n \angle \phi_s^n - jX_m I_r^n \angle \phi_r^n = 0 \quad (1b)$$

$$\left(\frac{R_r}{s} + j(X_r + X_m)\right) I_r^p \angle \phi_r^p - jX_m I_s^p \angle \phi_s^p = 0 \quad (1c)$$

$$\left(\frac{R_r}{2-s} + j(X_r + X_m)\right) I_r^n \angle \phi_r^n - jX_m I_s^n \angle \phi_s^n = 0 \quad (1d)$$

Further, the voltage of the motor terminals can be found:

$$V_t^p \angle \theta_g^p = -V_g^p \angle \theta_g^p + (R_m + j(X_s))I_s^p \angle \phi_s^p \quad (2)$$

$$V_t^n \angle \theta_g^n = -V_g^n \angle \theta_g^n + (R_g + j(X_s))I_s^n \angle \phi_s^n$$

The air gap power developed by the positive and negative sequence components are given in (3), with one to produce forward electromagnetic torque while the other to produce backward torque.

$$P_{ag}^p = 3(I_r^p)^2 \frac{R_r}{s}, P_{ag}^n = 3(I_r^n)^2 \frac{R_r}{(2-s)} \quad (3)$$

As a result of the two components of the air gap power, the electromagnetic torque of the motor will contain two components as given in (4).

$$T_{em}^p = \frac{\text{poles}}{2} \frac{P_{ag}^p}{\omega_e}, T_{em}^n = \frac{\text{poles}}{2} \frac{P_{ag}^n}{-\omega_e}, \quad (4)$$

$$T_{em} = T_{em}^p + T_{em}^n = \frac{\text{poles}}{2} \frac{3R_r}{\omega_e} \left[\frac{(I_r^p)^2}{s} - \frac{(I_r^n)^2}{(2-s)} \right]$$

A. Ripples in the torque

During the unbalanced condition of the stator, the magnitude of the three-phases and the angle displacements will not be the same. The positive and negative component of the stator current can be obtained by decomposing the three-phase currents using the symmetrical component theory. The positive sequence component of rotor current can be observe at frequency $\omega_r = \omega_e - \omega_m = s\omega_e$ while the negative sequence component are observe at frequency $-\omega_e - \omega_m = -(2-s)\omega_e$.

While interactions between stator and rotor currents in the same sequence produce torque of dc values, interactions between stator current and rotor current in difference sequences introduce ripples of 120 Hz. Detailed analysis can be referred in [15].

III. STEADY-STATE CALCULATION

Expressions (1a-1d), related to the motor circuits, constitute four complex algebraic equations which can be separated to 8 algebraic real equations as given in (5a-5h). Expression (5i) is related to the torque requirement. If the grid voltage and motor torque are given, there are nine unknown state variables, magnitudes and angles of rotor and stator positive- and negative-sequence currents and the slip rate. The nine unknown quantities of the motor can be found by solving the nine equations (5a-5i) using any well known iterative way such as Newton-Ralphson. In this paper, YALMIP is used to solve the nonlinear set of equations through nonlinear programming solver `fmincon`. Once the stator currents are found, the terminal voltages of the motor can be found using (5).

$$f_1 = -V_g^p \cos \theta_g^p + (R_s + R_g)I_s^p \cos \phi_g^p + X_m I_r^p \sin \phi_r^p - (X_s + X_m + X_g)I_s^p \sin \phi_s^p = 0 \quad (5a)$$

$$f_2 = -V_g^p \sin \theta_g^p + (R_s + R_g)I_s^p \sin \phi_g^p - X_m I_r^p \cos \phi_r^p + (X_s + X_m + X_g)I_s^p \cos \phi_s^p = 0 \quad (5b)$$

$$f_3 = \frac{R_r}{s} I_r^p \cos \phi_r^p - (X_r + X_m)I_r^p \sin \phi_r^p + X_m I_s^p \sin \phi_s^p = 0 \quad (5c)$$

$$f_4 = \frac{R_r}{s} I_r^p \sin \phi_r^p + (X_r + X_m)I_r^p \cos \phi_r^p - X_m I_s^p \cos \phi_s^p = 0 \quad (5d)$$

$$f_5 = -V_g^n \cos \theta_g^n + (R_s + R_g)I_s^n \cos \phi_g^n + X_m I_r^n \sin \phi_r^n - (X_s + X_m + X_g)I_s^n \sin \phi_s^n = 0 \quad (5e)$$

$$f_6 = -V_g^n \sin \theta_g^n + (R_s + R_g)I_s^n \sin \phi_g^n - X_m I_r^n \cos \phi_r^n + (X_s + X_m + X_g)I_s^n \cos \phi_s^n = 0 \quad (5f)$$

$$f_7 = \frac{R_r}{2-s} I_r^n \cos \phi_r^n - (X_r + X_m)I_r^n \sin \phi_r^n + X_m I_s^n \sin \phi_s^n = 0 \quad (5g)$$

$$f_8 = \frac{R_r}{2-s} I_r^n \sin \phi_r^n + (X_r + X_m)I_r^n \cos \phi_r^n - X_m I_s^n \cos \phi_s^n = 0 \quad (5h)$$

$$f_9 = T_{em} \frac{2\omega_e}{p} - 3I_r^p{}^2 \left[\frac{R_r}{s} \right] + 3I_r^n{}^2 \left[\frac{R_r}{(2-s)} \right] = 0 \quad (5i)$$

For the balanced voltage condition, only the set of equations related to the positive sequence circuit are used and the developed torque of the motor has only the positive component.

A. Initial values

Solving the set of the nonlinear equations (5a-5i) requires setting initial values for the decision variables. A large error in the initial values may cause the algorithm to converge to a local solution not desired. It may also cause non-convergence issues. A robust method to estimate the initial values is by obtaining the values of the variable at slip rate close to zero since it is the region where induction motor operates during

the steady state operation. In this literature, the initial values are obtained at slip equals to 0.1 as given in (6).

$$\begin{aligned} I_s^p \angle \phi_s^p &= \frac{V_g^p \angle \theta_r^p}{R_s + R_g + Z_p + jX_s + jX_g} \\ I_s^n \angle \phi_s^n &= \frac{V_g^n \angle \theta_r^n}{R_s + R_g + Z_n + jX_s + jX_g} \\ I_r^p \angle \phi_r^p &= \frac{jX_m I_s^p \angle \phi_s^p}{jX_m + jX_r + \frac{R_r}{0.1}} \\ I_r^n \angle \phi_r^n &= \frac{jX_m I_s^n \angle \phi_s^n}{jX_m + jX_r + \frac{R_r}{2-0.1}} \end{aligned} \quad (6)$$

$$\text{where } Z_p = \frac{(jX_r + \frac{R_r}{0.1})jX_m}{jX_r + \frac{R_r}{0.1} + jX_m}$$

$$Z_n = \frac{(jX_r + \frac{R_r}{2-0.1})jX_m}{jX_r + \frac{R_r}{2-0.1} + jX_m}$$

IV. CASE STUDIES

A. Case Study 1: Find The Motor State Variables During Unbalance Voltage Condition

To validate the proposed method in Section III, a testbed of an induction motor served by a voltage source is simulated in MATLAB/SimPowerSystems environment. The motor is connected to the grid bus through an RL circuit. The model parameters are shown in Table I. In the simulation model, the

TABLE I: model parameters

R_s	0.435(Ω)	friction factor	0
R_r	0.816(Ω)	pole pairs	2
L_s	4.0(mH)	Inertia	0.089
L_r	2.0(mH)	T_{mech}	11.9($N.m$)
L_m	69.31(mH)	V	220(60Hz)
R_g	0.1(Ω)	HP	3
L_g	1(mH)		

motor runs until it reaches the steady-state region. Then, an unbalanced voltage condition occurs where the voltage at phase *a* drops to 0.8 p.u. The stator voltages and currents during the voltage dip condition obtained from the simulation are shown in Fig. 3a and Fig. 3b, respectively. Fig. 3c shows the motor speed. In Table II, the simulation results are compared with the results using the proposed method described in section III. The input values to the optimization problem is the grid voltage (phase-a is 143.7V or 0.8 p.u) and the load Torque (11.9N.m). The algorithm required 4 iterations to find the solutions for the equations. Fig. 4 shows the rotor currents for phase A and

TABLE II: Motor variables

	Simulation	Proposed method
$I_s^p \angle \phi_s^p$	11.8148 \angle -37.2163	11.8145 \angle -37.2151
$I_s^n \angle \phi_s^n$	4.3057 \angle 109.5634	4.3010 \angle 109.5387
$V_t^p \angle \theta_t^p$	164.0435 \angle -0.9893	164.0438 \angle -0.9893
$V_t^n \angle \theta_t^n$	10.3024 \angle 179.2334	10.3043 \angle 179.2385
s	0.0548	0.0548
$I_r^p \angle \phi_r^p$	10.05 \angle -8.2253	10.0445 \angle -8.2268
$I_r^n \angle \phi_r^n$	4.1805 \angle 110.4117	4.1799 \angle 110.4327

the positive-and negative-component of the rotor current after

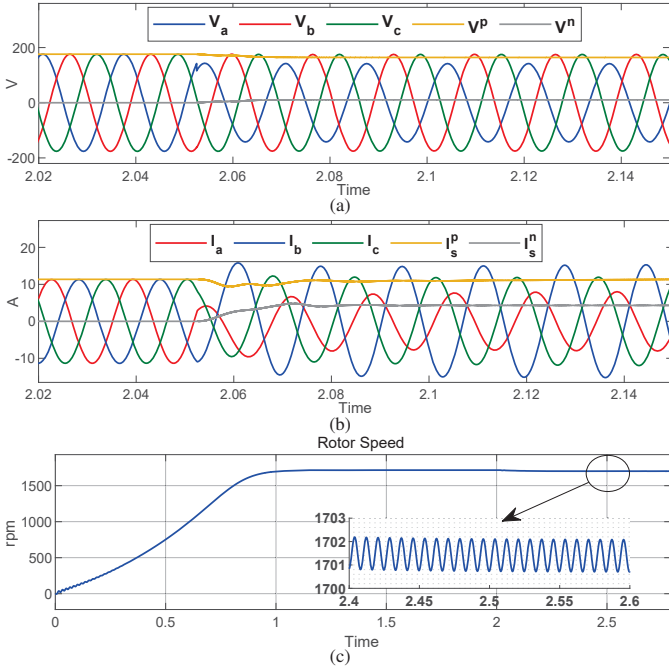


Fig. 3: Simulation results. (a) Stator voltages. (b) Stator currents. (c) Motor speed.

they are extracted. The positive-sequence of the rotor current rotates at frequency 3.2 Hz while the negative component has a frequency of 116.7 Hz. Table II shows the magnitude and angles of the positive and negative component of the rotor current obtained from the simulation and proposed method.

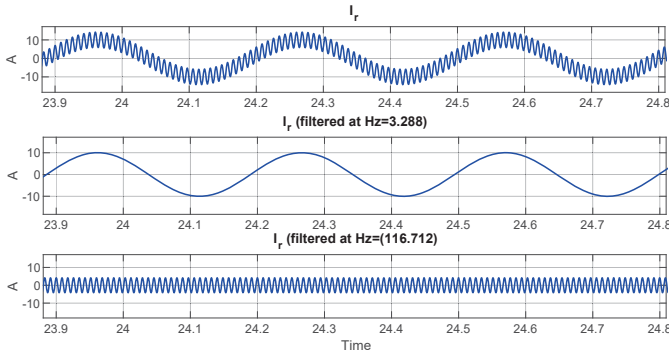


Fig. 4: Rotor currents of the induction motor.

B. Case Study 2: Maximum Torque During Unbalanced Voltage Dip

The maximum or breakdown torque is a function of the terminal voltage of the motor as shown in Fig. 5. As the terminal voltage drops, the maximum torque can be achieved by the motor decreases. During unbalanced voltage condition, the maximum load torque limit the induction motor can handle is reduced due to the reversing torque produced by the negative sequence current. When a motor reaches a steady state region during a voltage dip, the motor torque can be increased to a certain value or limit. Beyond this limit, the motor will go

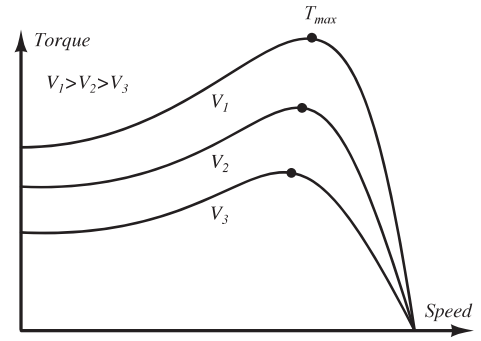


Fig. 5: Torque-speed curve of induction motor.

to the instability region where the steady state equations (5a-5i) can not be satisfied. For example, in Fig. 6, after the grid voltage dropped at $t = 1.5$ s, the motor reaches to the steady state region again and meet the load torque requirement. At $t = 2.5$ s, the load torque is increased. The motor is able to serve the given load torque since it is below the maximum breakdown point. At $t = 4$ s, the load torque is increased again. However, the load torque is more than the maximum torque capability of the motor during the voltage dip which leads the motor to the instability region. Fig. 6a shows the balanced voltage dip case, while Fig. 6b shows the unbalanced voltage case.

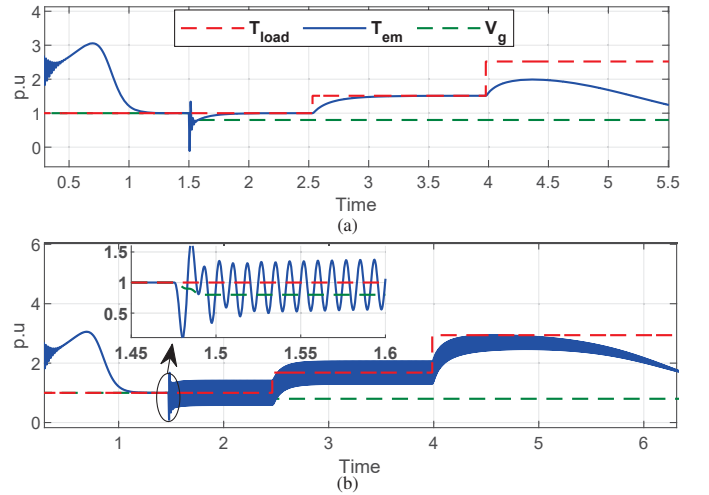


Fig. 6: Induction motor response to change in load torque. (a) Balanced voltage dip. (b) Unbalanced voltage dip.

To find the maximum torque limit during balanced and unbalanced voltage dip conditions, the optimization problem is formulated as in (7) and solved by `fmincon` through YALMIP. The objective function will be the maximization of the electromagnetic torque. The constraints of the optimization problem include the nine equations describing the circuits and torque, the slip limit, and the angle limits. The decision variables are the stator, rotor currents and the slip ($I_s^p, I_s^n, I_r^p, I_r^n, \phi_s^p, \phi_s^n, \phi_r^p, \phi_r^n, s$) while the input value to the

optimization problem is the grid voltage.

$$\begin{aligned}
 & \text{Maximize}(T_{em}) \\
 & \text{subject to (5)} \\
 & 1 \geq s \geq 0 \\
 & \pi \geq \phi_s^p, \phi_s^n, \phi_r^p, \phi_r^n \geq -\pi
 \end{aligned} \tag{7}$$

The maximum torque are found to be 23.5 and 32 N.m for the balanced and unbalanced voltage dip, respectively. To validate these limits, the load torque is set to values that are below the thresholds by 0.5 N.m at $t = 2.5$ s after the occurrence of the voltage dip at $t = 1.5$ s as shown in Fig. 7. At $t = 6$ s, the load torque is increased above the thresholds by 0.5 N.m. It can be seen that the motor loses its stability after crossing the given thresholds, while it is stable below them.

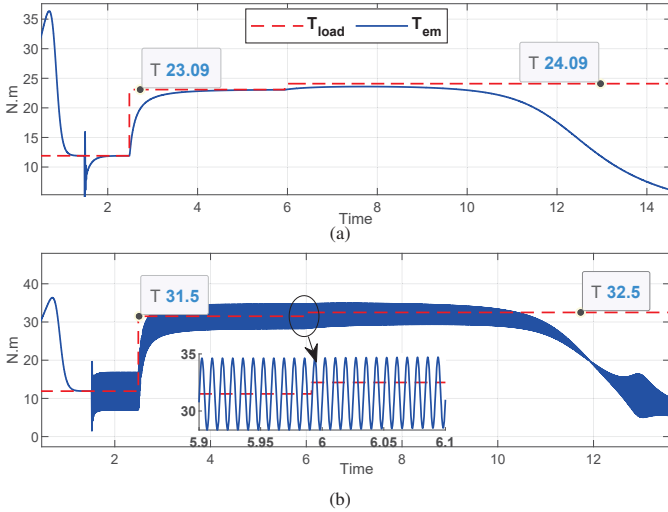


Fig. 7: Motor response for change in load torque above and below the threshold. (a) During balanced dip. (b) During unbalanced dip.

C. Case Study 3: Minimal Grid Voltage a Motor Can Handle For a Given Torque

Grid voltage drop may cause a motor stall. In this case study, we examine the minimal grid voltage a motor can handle for a given load torque. When the grid voltage dips, the motor voltage can be decreased as long as the steady state equation in(5a-5i) can be satisfied. Once these equations are not satisfied, the motor will lose its stability. In Fig. 8, the grid voltage decreases at $t = 1.5$ s. As a result, the stator current increases to meet the load requirement. At $t = 3$ s, the grid voltage dropped to a level that is less than the minimum voltage that the motor can handle which cases stability issues. To find the minimal grid voltage system can handle for a given torque, the optimization problem is formulated as in (8). The objective function will be the minimization of the grid voltage. The constrains of the optimization problem are the the steady state circuit and torque equations (5a-5d), the slip and angle limits. The input value to the optimization problem is the load

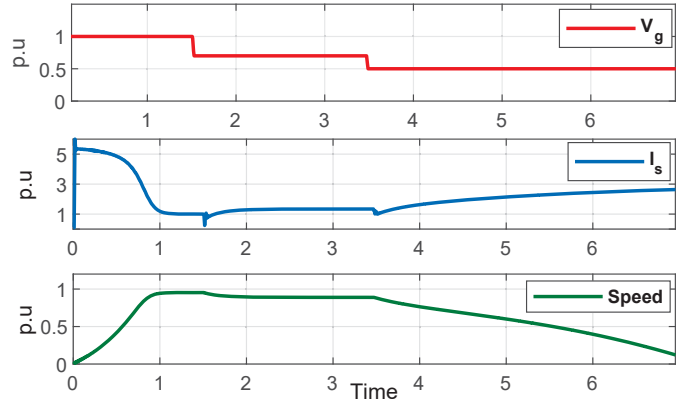


Fig. 8: Induction motor response to change in voltage.

torque of the motor and, the decision variables are the stator, rotor currents and the slip($I_s^p, I_r^p, \phi_s^p, \phi_r^p, s$).

$$\begin{aligned}
 & \text{Minimize}(V_g^p) \\
 & \text{Subject to (5a - 5d)} \\
 & T_{Load} \frac{2\omega_e}{\text{Poles}} - 3I_r^p \left[\frac{R_r}{s} \right] = 0 \\
 & 1 \geq s \geq 0 \\
 & \pi \geq \phi_s^p, \phi_r^p \geq -\pi
 \end{aligned} \tag{8}$$

By solving (8) for the given motor in Table I, the minimal grid voltage the motor can handle for 11.9 N.m load torque is 102 V (phase voltage). Fig. 9b shows the motor speed response to the change in grid voltage shown Fig. 9a. In case A, the grid voltage is set 1V below the threshold at $t = 1.5$ s while it is above the threshold by 1V in case B. It can be seen that, the motor becomes unstable when the grid voltage is below the boundary found by the proposed method.

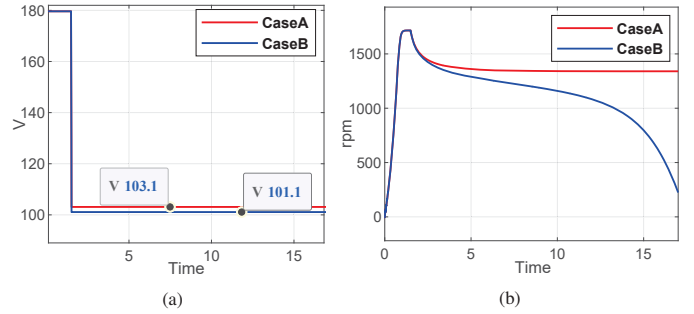


Fig. 9: Motor response. (a) Grid voltage. (b) Motor speed.

V. CONCLUSION

This paper has presented constrained nonlinear optimization algorithm to actually identify the maximum load torque for induction motor during a balanced and unbalanced voltage dip conditions that occur when the machine is in the steady-state operation. Moreover, the minimum voltage that can be achieved to serve a certain load torque is computed using an optimization-based approach. Additionally, the paper has presented an accurate method to obtain the steady-state electrical

variables of the induction motor for a give voltage and load torque by solving a set of nonlinear equations using fmincon algorithm. Exact equivalent circuit is used throughout the paper to obtain accurate results. The proposed approach is validated by comparing the results with the simulation results using Simulink environment.

REFERENCES

- [1] A. Jalilian and R. Roshanfekar, "Analysis of three-phase induction motor performance under different voltage unbalance conditions using simulation and experimental results," *Electric Power Components and Systems*, vol. 37, no. 3, pp. 300–319, 2009.
- [2] K. LeDoux, P. Visser, D. Hulin, and H. Nguyen, "Starting large synchronous motors in weak power systems," in *Industry Applications Society 60th Annual Petroleum and Chemical Industry Conference*. IEEE, 2013, pp. 1–8.
- [3] J. De Oliveira, L. Neto, and P. Ribeiro, "Power quality impact on performance and associated costs of three-phase induction motors," in *8th International Conference on Harmonics and Quality of Power. Proceedings (Cat. No. 98EX227)*, vol. 2. IEEE, 1998, pp. 791–797.
- [4] Y.-J. Wang, "An analytical study on steady-state performance of an induction motor connected to unbalanced three-phase voltage," in *2000 IEEE Power Engineering Society Winter Meeting. Conference Proceedings (Cat. No. 00CH37077)*, vol. 1. IEEE, 2000, pp. 159–164.
- [5] J. Williams, "Operation of 3-phase induction motors on unbalanced voltages [includes discussion]," *Transactions of the American Institute of Electrical Engineers. Part III: Power Apparatus and Systems*, vol. 73, no. 2, pp. 125–133, 1954.
- [6] J. C. Gomez, M. M. Morcos, C. A. Reineri, and G. N. Campetelli, "Behavior of induction motor due to voltage sags and short interruptions," *IEEE Transactions on Power Delivery*, vol. 17, no. 2, pp. 434–440, 2002.
- [7] E. Fuchs, D. Roesler, and F. Alashhab, "Sensitivity of electrical appliances to harmonics and fractional harmonics of the power system's voltage. part i: Transformers and induction machines," *IEEE Transactions on Power Delivery*, vol. 2, no. 2, pp. 437–444, 1987.
- [8] C.-Y. Lee, "Effects of unbalanced voltage on the operation performance of a three-phase induction motor," *IEEE Transactions on Energy Conversion*, vol. 14, no. 2, pp. 202–208, 1999.
- [9] M. Berndt and N. Schmitz, "Derating of polyphase induction motors operated with unbalanced line voltages," *Transactions of the American Institute of Electrical Engineers. Part III: Power Apparatus and Systems*, vol. 81, no. 3, pp. 680–683, 1962.
- [10] B. Gafford, W. Duesterhoeft, and C. Mosher, "Heating of induction motors on unbalanced voltages," *Transactions of the American Institute of Electrical Engineers. Part III: Power Apparatus and Systems*, vol. 78, no. 3, pp. 282–286, 1959.
- [11] J. R. Ramamurthy, S. Kolluri, D. J. Mader, and E. Camm, "Mitigation of motor starting voltage sags using distribution-class statcom," in *2018 IEEE/PES Transmission and Distribution Conference and Exposition (T&D)*. IEEE, 2018, pp. 1–9.
- [12] A. Von Jouanne and B. Banerjee, "Assessment of voltage unbalance," *IEEE transactions on power delivery*, vol. 16, no. 4, pp. 782–790, 2001.
- [13] F. Oliveira and A. Ukil, "Comparative performance analysis of induction & synchronous reluctance motors in chiller systems for energy efficient buildings," *IEEE Transactions on Industrial Informatics*, 2019.
- [14] J. Lofberg, "Yalmip: A toolbox for modeling and optimization in matlab," in *Computer Aided Control Systems Design, 2004 IEEE International Symposium on*. IEEE, 2004, pp. 284–289.
- [15] L. Fan, S. Yuvarajan, and R. Kavasseri, "Harmonic analysis of a dfig for a wind energy conversion system," *IEEE Transactions on Energy Conversion*, vol. 25, no. 1, pp. 181–190, 2010.